Comparison of Dielectric and Viscoelastic Relaxation Functions of *cis*-Polyisoprenes: Test of Tube Dilation Molecular Picture

Y. Matsumiya, H. Watanabe,* and K. Osaki

Institute for Chemical Research, Kyoto University, Uji, Kyoto 611-0011, Japan

Received July 13, 1999

ABSTRACT: Within the context of the generalized tube model, the tube representing the entanglement constraint is not necessarily fixed in space but moves with time. This tube motion results in constraint release (CR) as well as dynamic tube dilation (DTD) for the chain trapped in the tube. For monodisperse systems, the DTD molecular picture leads to the normalized relaxation modulus $\mu(t)$ ($=G(t)/G_N$) being proportional to square of the surviving fraction of the dilated tube. In contrast, the normalized dielectric relaxation function $\Phi(t)$ of the chain having noninverted type-A dipoles is proportional to this fraction. Thus, the viscoelastic and dielectric relaxation functions satisfy a relationship $\mu(t) = [\Phi(t)]^2$ if the tube dilates in time scales of the chain relaxation. The validity of this relationship was examined for linear *cis*-polyisoprene (PI) chains having those type-A dipoles. The relationship was approximately valid, and thus, the tube dilated for the PI chains with $M/M_e = 10-30$ in their bulk state, although these chains did not necessarily reptate in the dilated tube with their intrinsic curvilinear diffusion coefficient. On the other hand, the relationship reformulated for blends was not valid for dilute PI probe chains in entangling matrices of much shorter polybutadiene (PB) chains. The probe fully relaxed via the CR mechanism during the DTD process and did not obey this relationship. The lack of DTD was also confirmed for the same probe in a much longer, CR-free PB matrix.

1. Introduction

Many molecular models have been developed in attempt to describe the motion of entangled chains and the corresponding properties, e.g., the zero-shear viscosity η_0 of linear chains that is proportional to ≅3.5th power of the molecular weight M.[1,2] Among those models, the tube models[3−16] seem to be most successful in the sense that viscoelastic and other dynamic properties are consistently calculated from the simplified chain motion assumed in the models.

In the tube models, the entanglement is represented as an uncrossable tube and the chain moves under the constraint from this tube. The original Doi−Edwards (DE) model[3,4] assumed that the tube is fixed in space and the linear chain therein has a constant contour length at equilibrium. The resulting, simple reptation motion can qualitatively explain the dynamic properties of entangled linear chains. However, nontrivial differences between the DE predictions and experiments are noted for many properties, e.g., the M dependence of η_0 and the distribution of terminal viscoelastic modes, the latter characterized by a product of the steady-state recoverable compliance J_e and the entanglement plateau modulus G_N. Thus, attempts have been made to generalize/refine the tube model by incorporating various dynamic modes not considered in the DE model, e.g., the contour length fluctuation (CLF)[7,8] that is similar in some ways to the arm retraction mode[5,6] considered for star chains, the constraint release (CR)[9,10] that allows the tube and the chain therein to move over a large distance in a direction perpendicular to the chain contour, and the dynamic tube dilation (DTD)[11] that increases the tube diameter (as a result of CR). Refined models combining these modes with the reptation/arm retraction modes can describe the behavior of entangled chains with considerable accuracy.[12−17] Some details of these models (including their limitations) and results of comparison with experiments are summarized in a recent review.[18]

This paper focuses on the DTD mechanism at equilibrium (in the linear response regime). The stress partially relaxes when the chain explores all local configurations in the dilated tube, and the terminal relaxation is accelerated if the chain reptates/retracts along the dilated and shortened tube with its intrinsic curvilinear diffusion coefficient. For the relaxation of star chains, the importance of DTD combined with the arm retraction was suggested by Ball and McLeish[12] and by Milner and McLeish.[13,14] For linear chains, the validity of DTD combined with reptation is sometimes questioned.[12,19] However, the tube dilation process itself has been neither verified nor disproved from experiments for systems in which the tube can, in principle, dilate in time scales of the chain relaxation.

For this problem, we note an interesting possibility of testing the DTD molecular picture through comparison of viscoelastic and dielectric properties. For a chain having so-called type-A dipoles[20] that are parallel along its backbone, the global motion is differently reflected in these properties and the comparison enables us to extract some detailed information for this motion.[21] In fact, the comparison on the basis of the eigenmode analysis revealed that the entanglement in monodisperse systems provides the chain with some degree of coherence in its subchain motion[21] and that the CR mechanism tends to decrease this coherence.[22,23]

For the experimental examination of the DTD picture, the purpose of this paper, we have derived a specific relationship between the viscoelastic and dielectric properties that should hold if the tube dilates in time scales of the chain relaxation. Furthermore, we have tested this relationship for linear *cis*-polyisoprene (PI) chains having the noninverted type-A dipoles and found that the tube actually dilates in monodisperse systems. The results are summarized in this paper.

2. Theoretical Background

2.1. Monodisperse Systems. *2.1.1. General.* We consider a monodisperse system of linear Gaussian

10.1021/ma991121q CCC: $19.00
Published on Web 01/08/2000

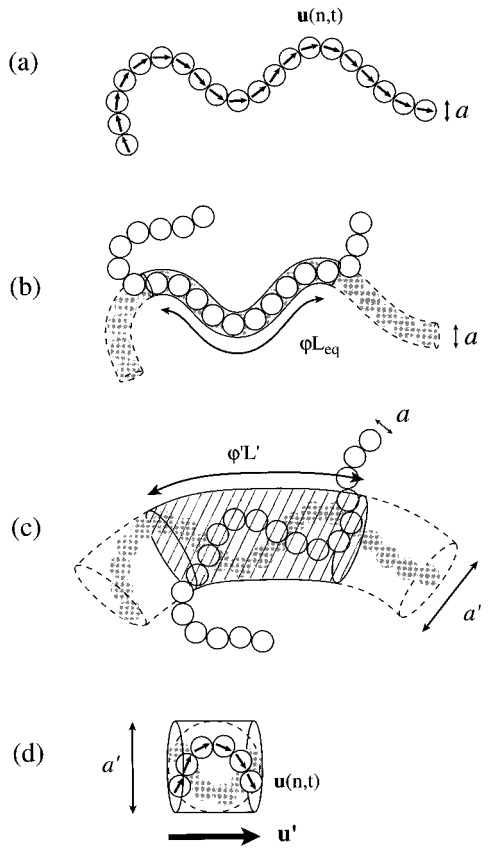

Figure 1. Schematic illustration of the chain and tube. In all parts a−d, filled (shaded) and unfilled circles indicate the entanglement segments (of size a) at times 0 and t, respectively. (a) Bond vectors (arrows) of the entanglement segments of the chain. (b) Chain reptating in the fixed tube of diameter a. (c) Chain in the dilated (enlarged) tube of diameter a'. The hatched portion of the initial, enlarged tube contains the chain at time t. (d) Combination of entanglement segments into a larger, coarse-grained segment having the bond vector $\mathbf{u}'$ (thick long arrow).

chains each composed of N entanglement segments ($N = M/M_e$, with M_e being the molecular weight between entanglements). The chain has the noninverted type-A dipoles. The bond vector (end-to-end vector) of the nth entanglement segment at a time t is denoted by $\mathbf{u}(n,t)$; $\mathbf{u}$ has an equilibrium size $a = \langle \mathbf{u}^2 \rangle_{eq}^{1/2}$ ($\propto M_e^{1/2}$); see Figure 1a.

We consider the chains subjected to a small step shear strain γ (in the linear viscoelastic regime) at $t = 0$. The stress−optical rule allows us to express the shear relaxation modulus $G(t)$ as[4,21,24]

$$G(t) = \frac{3\nu k_B T}{\gamma} \sum_{n=1}^{N} S(n,t) \tag{1}$$

with

$$S(n,t) = \frac{1}{a^2} \langle u_x(n,t) u_y(n,t) \rangle \tag{2}$$

Here, ν is the chain number density in the system, k_B is the Boltzmann constant, and T is the absolute temperature. (In eq 2, the shear and shear gradient directions are chosen to be in the x and y directions, respectively.) The *orientation function*, $S(n,t)$, represents the isochronal orientational anisotropy of individual entanglement segments.

Utilizing the Doi−Edwards initial condition,[3,4] $S(n,0) = S_0 = 4\gamma/15$ (for $\gamma \ll 1$), we can rewrite eq 1 as

$$G(t) = G_N \mu(t) \tag{3}$$

with

$$G_N = \frac{4\nu N k_B T}{5} \quad \text{and}$$

$$\mu(t) = \frac{1}{N S_0} \sum_{n=1}^{N} S(n,t) \; (\mu(0) = 1) \tag{4}$$

Here, $\mu(t)$ is the normalized relaxation modulus. The initial condition for the affine deformation, $S(n,0) = S_0 = \gamma/3$, also gives eqs 3 and 4 except that the numerical factor for G_N, $^4/_5$ in eq 4, becomes unity.

The normalized dielectric relaxation function $\Phi(t)$ is given by an autocorrelation of the polarization of the system.[25] For the chain having noninverted type-A dipoles, a sum of the dipoles in the nth entanglement segment is proportional to $\mathbf{u}(n,t)$. Thus, $\Phi(t)$ of these chains at equilibrium (in the linear response regime) is written as[21,26]

$$\Phi(t) = \frac{1}{N} \sum_{n=1}^{N} \sum_{m=1}^{N} C(n,t;m) \; (\Phi(0) = 1) \tag{5}$$

with

$$C(n,t;m) = \frac{1}{a^2} \langle \mathbf{u}(n,t) \cdot \mathbf{u}(m,0) \rangle \; (C(n,0;m) = \delta_{nm}) \tag{6}$$

The *local correlation function*, $C(n,t;m)$, detects orientational correlation of two entanglement segments in individual chains at two separate times t and 0. (Cross-correlation of different chains vanishes on average and does not contribute to $\Phi(t)$ when the dipole−dipole interaction energy is much smaller than the thermal energy $k_B T$.[26] This is the case for PI chains having only small dipoles.)

Changes of $S(n,t)$ and $C(n,t;m)$ with t, which result in the viscoelastic and dielectric relaxation (decay of $G(t)$ and $\Phi(t)$), are commonly determined by the chain motion. However, this motion is differently reflected in S and C, the former detecting the *isochronal* orientational anisotropy and the latter, the orientational correlation *at two separate times*. Thus, the relationship between the viscoelastic and dielectric quantities calculated from $G(t)$ and $\Phi(t)$ (i.e., from S and C) changes with the type of the chain dynamics.[21−23] This in turn enables us to specify some details about the chain motion in a particular system from the observed relationship.

2.1.2. Relaxation Functions of Fixed Tube Model. In the models assuming the spatially *fixed* tube, the viscoelastic $\mu(t)$ and dielectric $\Phi(t)$ are expressed in terms of the tube survival fraction $\varphi(t)$ as[4−8]

$$\mu(t) = \Phi(t) = \varphi(t) \text{ (for the case of fixed tube)} \tag{7}$$

For convenience of the later formulation of $\mu(t)$ and $\Phi(t)$ for the chain in the dilated tube, we here summarize how eq 7 is derived from the more fundamental expressions of μ and Φ, i.e., eqs 4 and 5.

We consider that the initial tube (the tube at $t = 0$) contains successive $q + 1$ entanglement segments

(indexed from n^* to $n^* + q$) of the chain at the time t; see Figure 1b. These segments have configurations identical to those of the initial segments indexed from m^* to $m^* + q$, i.e.,

$$\mathbf{u}(n^* + p, t) = \mathbf{u}(m^* + p, 0) \qquad (p = 0, 1, 2,.., q) \quad (8)$$

The other segments at the time t have escaped from the initial tube, and their $\mathbf{u}(n,t)$ are isotropically distributed and not correlated with the initial chain configuration. For this case, eqs 2 and 6 become

$$S(n,t) = S_0 \qquad \text{for } n^* \le n \le n^* + q \qquad (9a)$$

$$S(n,t) = 0 \qquad \text{for the other } n \text{ values} \qquad (9a)$$

and

$$C(n,t;m) = \langle \mathbf{u}^2 \rangle_{eq}/a^2 = 1 \quad \text{for } m = n + m^* - n^* \text{ and } n^* \le n \le n^* + q \quad (10a)$$

$$C(n,t;m) = 0 \qquad \text{for the other } n \text{ and } m \text{ values} \quad (10b)$$

Utilizing these results in eqs 4 and 5 and considering the definition of the tube survival fraction, $\varphi(t) = (q + 1)/N$, we obtain eq 7. (In this derivation, the chain is implicitly assumed to have a constant contour length $L_{eq} = Na$ and the surviving portion of the tube has the length φL_{eq}; see Figure 1b. However, eq 7 can be also deduced without this assumption.[4])

2.1.3. Survival Fraction of Dilating Tube. Marrucci[11] first formulated a model for the tube dilation. The dilated tube, defined at respective t, is composed of $N'(t)$ enlarged segments of the size $a'(t)$ (=dilated tube diameter), and each enlarged segment includes $\beta(t)$ entanglement segments, where $N'(t) = Na^2/[a'(t)]^2$ and $\beta(t) = [a'(t)]^2/a^2$.

The surviving fraction $\varphi'(t)$ of the dilated (enlarged) tube segments, the central quantity in the Marrucci model,[11] is defined in the way schematically explained in Figure 1c. The filled (shaded) and unfilled circles indicate the entanglement segments of the chain at times 0 and t, respectively. The dilated tube at the time t has the diameter $a' = \beta^{1/2}a$. As a reference for this tube, we combine each β entanglement segments *at time 0* into an enlarged segment to define the *initial*, enlarged tube of the diameter a' and length L' (=a'N'). At the time t, the hatched portion of this initial, enlarged tube still contains the chain (i.e., the constraint due to this portion survives). The $\varphi'(t)$ is defined as a ratio, L_s'/L', where L_s' is the length of this surviving portion. ($N\varphi'$ entanglement segments are included in that portion.)

2.1.4. Relaxation Modulus of Tube Dilation Model. Marrucci[11] utilized the total number of the dilated segments $N'(t)$ and their survival fraction $\varphi'(t)$ to express the relaxation modulus of the monodisperse system as

$$G(t) = \frac{4}{5}\nu k_B T N'(t)\varphi'(t) \qquad (11)$$

This expression is identical to that for the cases of the fixed tube, $G(t) = 4\nu k_B T N \varphi(t)/5$ (eqs 3, 4, and 7), *except* that eq 11 includes N' and φ' of the dilated segments instead of N and φ. In other words, in eq 11, the $\beta(t)$ entanglement segments (of size a) are fully coarse-grained into one dilated segment of size $a'(t)$ (=$[\beta(t)]^{1/2}a$ = $[N/N'(t)]^{1/2}a$). Validity of this coarse-graining is later discussed in relation to mutual equilibration of the $\beta(t)$ entanglement segments.

Marrucci[11] further considered that the fully relaxed portion of the chain (the portion out of the initial, enlarged tube; cf. Figure 1 c) behaves as a solvent. Then, φ' is analogous to the polymer concentration in usual solutions, and the diameter of the dilated tube is written as $a'(t) = a[\varphi'(t)]^{-\alpha/2}$ with $\alpha = 1-1.3$ (α = scaling exponent for the entanglement mesh size in solutions[1,2]). Correspondingly, $N'(t)$ is given by

$$N'(t) = N[\varphi'(t)]^{\alpha} \qquad (12)$$

From eqs 11 and 12, we obtain the Marrucci expression[11] of $\mu(t)$

$$\mu(t) = G(t)/G_N = [\varphi'(t)]^{1+\alpha} \qquad (13)$$

The same expression is deduced also from the relaxation modulus for the case of initial affine deformation, $G(t) = \nu k_B T N'(t)\varphi'(t)$. (Note that $G(t)$ given by eq 11 is based on the DE initial condition).

2.1.5. Validity of Coarse-Graining. Here, we examine a relationship between the Marrucci expression of $G(t)$, eq 11, and the stress−optical rule. For this purpose, we combine every successive β segment into an enlarged segment having the bond vector $\mathbf{u}'$ (cf. Figure 1d),

$$\mathbf{u}'(i,t) = \sum_{n=1+(i-1)\beta}^{i\beta} \mathbf{u}(n,t) \qquad i = 1, 2,..., N'(=N/\beta) \quad (14)$$

If the β entanglement segments are mutually equilibrated within a time scale of our observation t_{ob}, i.e., if they explore all possible local configurations in the enlarged segment within times $< t_{ob}$ (as schematically shown in Figure 1d), their bond vectors can be generally written as

$$\mathbf{u}(n,t_{ob}) = \frac{1}{\beta}\mathbf{u}'(i,t_{ob}) + \mathbf{v}(n,t_{ob}) \qquad (1 + (i-1)\beta \le n \le i\beta) \quad (15)$$

Here, $\mathbf{v}$ is an isotropically distributed random vector uncorrelated with $\mathbf{u}'$. Then, the stress−optical rule indicates that the shear stress sustained by the β entanglement segments is given by (cf. eqs 1 and 2)

$$\sigma = 3k_B T \sum_{n=1+(i-1)\beta}^{i\beta} \frac{1}{a^2}\langle u_x(n,t_{ob})u_y(n,t_{ob})\rangle = 3k_B T\left[\frac{1}{\beta a^2}\langle u'_x(i,t_{ob})u'_y(i,t_{ob})\rangle\right] \qquad (16)$$

This σ is identical to the stress of the enlarged (dilated) segment having the average size $a' = \beta^{1/2}a$. Namely, the β entanglement segments behave as an enlarged stress-generating unit as a whole if they are mutually equilibrated. For this case, $G(t)$ is evaluated in the same way as that in the fixed tube case, except that the enlarged segments are utilized as the structural unit instead of the smaller entanglement segments (of the size a), i.e., by use of the total number of the dilated segments N' (=N/β), their orientation function $S'(i,t) = (a')^{-2}\langle u'_x(i,t)u'_y(i,t)\rangle$, and the survival fraction φ' instead of N, $S(n,t)$, and φ. The resulting $G(t)$ (with the DE initial condition for S') is identical to that given by eq 11, the Marrucci expression.

This result demonstrates that eq 11 and its consequence, eq 13, are valid in time scales where the $\beta(t)$

entanglement segments are mutually equilibrated. This equilibration results from accumulation of local CR processes over the $\beta(t)$ entanglement segments and requires a time $\tau^{**} \sim [\beta(t)]^2 t_w$ (t_w = entanglement lifetime),[18] meaning that eqs 11 and 13 are consistent with the stress−optical rule in the time scale longer than τ^{**}. In addition, the molecular picture of the dilated tube makes sense only when N' of this tube is well above unity,[11] i.e., in the time scale $< \tau_{max}$ (the longest relaxation time of the system). Thus, eqs 11 and 13 are valid at $\tau^{**} < t < \tau_{max}$. (This argument of validity applies not only to the monodisperse systems but also to blends examined later.)

The chain has an intrinsic curvilinear diffusion coefficient, $D_c = N\zeta/k_BT$ (ζ = friction coefficient of the entanglement segment).[4] Marrucci[11] assumed the reptation of the chain with this D_c along the dilated tube to obtain explicit expressions of $\varphi'(t)$ and $\mu(t)$. The assumption of pure reptation is valid only in time scales longer than that for equilibration of the contour length measured along the dilated tube.[18] Thus, this assumption is not necessarily valid in time scales shorter than $\tau_{CR} \sim N^2 t_w$ (global CR time).[18] However, the tube dilates (to the diameter $a'(t) = [\beta(t)]^{1/2}a$) and the Marrucci expression of $G(t)$ (eq 11) is valid in time scales $> \tau^{**}$ irrespective of this assumption, i.e., even if the chain does not reptate with its intrinsic D_c along the dilated tube.

2.1.6. Dielectric Relaxation Function of Tube Dilation Model. Marrucci[11] did not examine the dielectric properties of the chains (having the noninverted type-A dipoles). However, we can utilize his concept to readily calculate the dielectric relaxation function $\Phi(t)$.

As noted from eqs 5 and 6, we can express $\Phi(t)$ of these chains in terms of the bond vectors of the *enlarged* (dilated) segments $\mathbf{u}'$ (eq 14) as

$$\Phi(t) = \frac{1}{N'(a')^2}\sum_{i=1}^{N'}\sum_{j=1}^{N'}\langle \mathbf{u}'(i,t)\cdot\mathbf{u}'(j,0)\rangle \qquad \text{with } (a')^2 = \beta a^2 \quad (17)$$

This result is obtained from a simple rearrangement of the summation in eq 5,

$$\sum_{n=1}^{N} \rightarrow \sum_{i=1}^{N'}\sum_{n=1+(i-1)\beta}^{i\beta}$$

Thus, eq 17 holds in any time scale ($<\tau_{max}$), irrespective of the mutual equilibration of the successive β entanglement segments. This feature of $\Phi(t)$ is different from the feature of $G(t)$: The equilibration itself does not change the $\Phi(t)$ value but decreases the $G(t)$ value by the factor $\beta^{-1} = N'/N$ (cf. eq 16). This difference between $\Phi(t)$ and $G(t)$ is related to a fact that correlation of different segments is included in $\Phi(t)$ but not in $G(t)$, the latter detecting a sum of orientational anisotropy of individual segments; see eqs 3−6.

From the above validity of eq 17, we can always choose the size of the enlarged segment to be identical to the dilated tube diameter under the situation depicted in Figure 1c and use these segments as the structural unit. Then, $\Phi(t)$ is evaluated in the same way as in the case of the fixed tube, except that N, $C(n,t;m)$, and φ are replaced by N' ($=N/\beta$), $C'(i,t;j) = (a')^{-2}\langle \mathbf{u}'(i,t)\cdot\mathbf{u}'(j,0)\rangle$, and φ'. (This situation is similar to that for $G(t)$.) The resulting expression of $\Phi(t)$ is

$$\Phi(t) = \frac{1}{N'}\sum_{i}'\sum_{j'}'\delta_{ij'} = \varphi' \qquad (18)$$

where the summation Σ' is taken for the enlarged segments in the surviving portion of the dilated tube shown in Figure 1c. (In eq 18, j' is equal to $j - j^* + i^*$. Here, j indexes the enlarged segments at the time 0, and j^* and i^* specify the segments at the edge of the surviving portion at the times 0 and t; j^* and i^* correspond to m^* and n^* in eq 8.)

From eqs 13 and 18, we find a relationship between the dielectric and viscoelastic properties of the chain in the dilated tube,

$$\mu(t) = [\Phi(t)]^{1+\alpha} \cong [\Phi(t)]^2 \quad \text{for } \alpha = 1 \quad (t < \tau_{max}) \quad (19)$$

Considering the viscoelastic and dielectric mode distributions of the chain, we can further rewrite eq 19 for the dielectric loss $\epsilon''(\omega)$ and complex modulus $G^*(\omega) = G'(\omega) + iG''(\omega)$ ($i = (-1)^{1/2}$) at the angular frequency ω. (ϵ'' and G* are given as the Fourier transformation of Φ and μ.) For the case of $\alpha = 1$, the result is simply written as

$$\frac{\epsilon''(\omega)}{\Delta\epsilon} = \sum_p g_p \frac{\omega\tau_p}{1+\omega^2\tau_p^2} \qquad (20)$$

and

$$\frac{G'(\omega)+iG''(\omega)}{G_N} = \sum_{p,q} h_{pq}\frac{\omega^2\tau_{pq}^2 + i\omega\tau_{pq}}{1+\omega^2\tau_{pq}^2} \qquad (21)$$

with

$$h_{pq} = g_p g_q \qquad \text{and } \tau_{pq} = [\tau_p^{-1} + \tau_q^{-1}]^{-1} \qquad (22)$$

Here, $\Delta\epsilon$ is the dielectric relaxation intensity due to the global motion of the chain. The $\epsilon''(\omega)$ and G*(ω) should satisfy the relationship specified by eqs 20−22 when the tube actually dilates in the time scale of the chain relaxation.

Because eqs 20−22 are deduced from the general arguments for the expressions of $\Phi(t)$ and $G(t)$, these equations are valid whenever the tube dilates in the time scale of the chain relaxation ($t < \tau_{max}$). In other words, eqs 20−22 hold not only for the Marrucci model but also for other models considering the chain that is in the dilated tube but does not reptate along this tube with the intrinsic D_c ($=N\zeta/k_BT$), e.g., the model of Viovy et al.[19] This point is later discussed in more details in relation to the data shown in Figures 2-4.

2.2 Blends. Now, we turn our attention to blends of probe and matrix chains, each composed of N_2 and N_1 entanglement segments and having number fractions of these segments v_2 and v_1, respectively. The probe and matrix chains may be chemically different, but they are uniformly mixed and entangled with each other. (The v_i reduces to the volume fractions of the probe and matrix chains if these chains are chemically identical.) Either the probe or matrix chains, or both, have the noninverted type-A dipoles. The survival fractions of the dilated tubes for the probe and matrix, $\varphi_2'(t)$ and $\varphi_1'(t)$, are defined in the way explained in Figure 1c. The average survival fraction is given by $\varphi'(t) = v_1\varphi_1'(t) +$

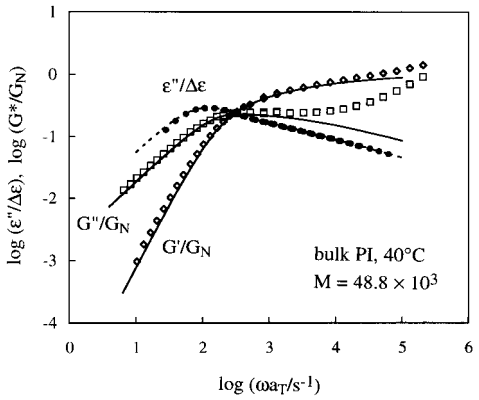

Figure 2. Normalized viscoelastic modulus G^*/G_N and dielectric loss $\epsilon''/\Delta\epsilon$ of a monodisperse bulk PI system with $M = 48.8 \times 10^3$ at 40 °C (symbols). The dotted curve shows the $\epsilon''/\Delta\epsilon$ recalculated from the dielectric spectrum (eq 20), and the solid curves indicate the $G^*(\omega)/G_N$ calculated from the same spectrum for the case of tube dilation (eqs 21 and 22). For more details, see text.

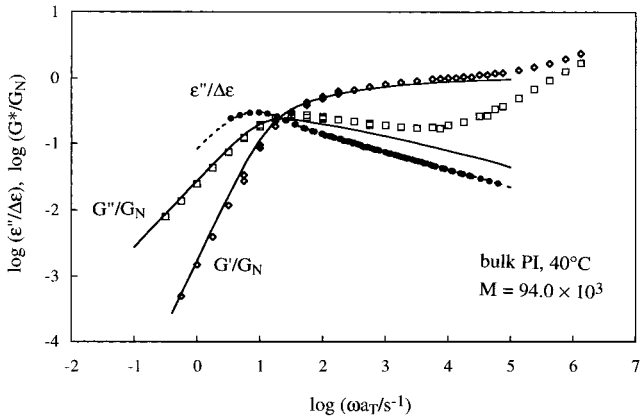

Figure 3. Normalized viscoelastic modulus G^*/G_N and dielectric loss $\epsilon''/\Delta\epsilon$ of a monodisperse bulk PI system with $M = 94.0 \times 10^3$ at 40 °C (symbols). The dotted curve shows the $\epsilon''/\Delta\epsilon$ recalculated from the dielectric spectrum (eq 20), and the solid curves indicate the $G^*(\omega)/G_N$ calculated from the same spectrum for the case of tube dilation (eqs 21 and 22). For more details, see text.

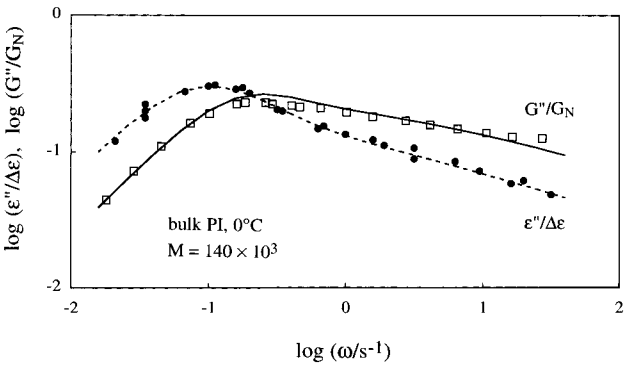

Figure 4. Normalized viscoelastic and dielectric losses G''/G_N and $\epsilon''/\Delta\epsilon$ of a monodisperse bulk PI system with $M = 140 \times 10^3$ at 0 °C (symbols). (Data reported by Adachi et al.[28] were normalized in this study.) The dotted curve shows the $\epsilon''/\Delta\epsilon$ recalculated from the dielectric spectrum (eq 20), and the solid curve indicates the $G''(\omega)/G_N$ calculated from the same spectrum for the case of tube dilation (eqs 21 and 22). For more details, see text.

$v_2\varphi_2'(t)$. For simplicity, we utilize the dilation exponent $\alpha = 1$ in the following discussion.

Considering that the numbers of the dilated tube segments for the probe and matrix are commonly determined by the average $\varphi'(t)$ in the way described by eq 12, we may express the relaxation modulus of the blend as[11]

$$G(t) = G_N[v_1\mu_1(t) + v_2\mu_2(t)] \quad \text{with } \mu_i(t) = \varphi'(t)\varphi_i'(t)\ (t < \tau_{max}) \quad (23)$$

Here, $\mu_i(t)$ is the normalized relaxation modulus of the component i ($i = 1$ and 2 for the matrix and probe). Irrespective of the details of the chain dynamics, eq 23 (derived by Marrucci for blends of chemically identical chains[11]) is consistent with the stress−optical rule in time scales longer than that for the *mutual equilibration* of entanglement segments in the dilated tube segment. (This situation is similar to that explained for the monodisperse systems.)

The normalized dielectric relaxation function of the blend is obtained from the argument similar to that for the monodisperse system. The result is

$$\Phi(t) = \tilde{v}_1\Phi_1(t) + \tilde{v}_2\Phi_2(t) \qquad \text{with } \Phi_i(t) = \varphi_i'(t) \quad (24)$$

Here, $\Phi_i(t)$ and $\tilde{v}_i$ are the dielectric relaxation function and intensity coefficient of the component i, the latter being defined by

$$\tilde{v}_i = \frac{v_i\xi_i}{v_1\xi_1 + v_2\xi_2} \qquad (i = 1,2) \quad (25)$$

In eq 25, ξ_i represents the squared magnitude of type-A dipoles per entanglement segment of the component i ($\xi_i = 0$ if this component has no type-A dipoles). The $\tilde{v}_i$ reduces to v_i if the probe and matrix are chemically identical.

Equations 23 and 24 specify the relationship between the viscoelastic and dielectric properties of the blend in which the tube dilates with t. We hereafter focus on a special class of blends in which the probe is very dilute and entangled only with the matrix chains and only the probe has the type-A dipoles ($\xi_1 = 0$ in eq 25). The dilute probes have no effect on the behavior of the matrix chains and do not contribute to the average survival fraction $\varphi'(t)$. Thus, under an assumption that the entanglement segments of the probe are *immediately* equilibrated on removal of topological constraints due to the matrix chains, eqs 23 and 24 are rewritten as

$$\mu_2(t) = \varphi'(t)\varphi_2'(t) \cong \varphi_{1,m}'(t)\varphi_2'(t) = [\mu_{1,m}(t)]^{1/2}\varphi_2'(t) \quad (26)$$

$$\Phi(t) = \Phi_2(t) = \varphi_2'(t) \quad (27)$$

In eq 26, we have replaced $\varphi'(t)$ by the survival fraction $\varphi_{1,m}'(t)$ in the monodisperse matrix system and further utilized eq 13 (with $\alpha = 1$) to rewrite $\varphi_{1,m}'(t)$ in terms of the normalized relaxation modulus $\mu_{1,m}(t)$ of the pure matrix.

From eqs 26 and 27, we find a relationship between the viscoelastic and dielectric properties of the dilute type-A probes in the dilated tube,

$$\mu_2(t) = [\mu_{1,m}(t)]^{1/2}\,\Phi_2(t) \qquad (t < \tau_{max}) \quad (28)$$

This result can be rewritten for ϵ_2'' and G_2^* of the probe: If the dielectric modes of the probe have the

relaxation times and intensities τ_p and g_p specified by eq 20 (with $\Delta\epsilon$ being the total intensity due to the global probe motion), the modulus G_2* of the probe in the dilated tube should be written as

$$\frac{G_2'(\omega) + iG_2''(\omega)}{G_{N_2}} = \sum_{p,q} \tilde{h}_{pq} \frac{\omega^2 \tilde{\tau}_{pq}^{\,2} + i\omega\tilde{\tau}_{pq}}{1 + \omega^2 \tilde{\tau}_{pq}^{\,2}} \quad (29)$$

with

$$\tilde{h}_{pq} = g_p r_q \qquad \text{and } \tilde{\tau}_{pq} = [\tau_p^{-1} + \tau_{r,q}^{-1}]^{-1} \quad (30)$$

Here, G_{N_2} ($=v_2 G_N$) is the probe contribution to the plateau modulus, and $\tau_{r,q}$ and r_q are the characteristic times and intensities for the relaxation modes of $[\mu_{1,m}(t)]^{1/2}$.

3. Experimental Section

A linear *cis*-polyisoprene (PI) was synthesized via anionic polymerization. The initiator and solvent were *sec*-butyllithium and heptane. The molecular weight and polydispersity index determined from GPC (HLC-802UR, Tosoh) combined with a low-angle laser light scattering photometer (LS-8000, Tosoh) were $M = 94.0 \times 10^3$ and $M_w/M_n = 1.05$, respectively. For this PI, linear viscoelastic and dielectric measurements were conducted with a rheometer (ARES, Rheometrics) and a transformer bridge (model 1620A, QuadTech). The time−temperature superposition[1] worked very well for the dielectric and viscoelastic data (with the same shift factor a_T). These data are reduced at 40 °C and compared with the previous data.[22,26,27]

For the other, previously examined PI sample ($M = 48.8 \times 10^3$, $M_w/M_n = 1.05$),[21,23,26] ϵ'' and G* were again measured in this study. The results excellently agreed with the previous data.[21,23,26]

4. Results and Discussion

As explained for eq 4, the proportionality constant between G_N and N ($=M/M_e$) changes a little according to our choice of the initial condition for $S(n,t)$ (the Doi−Edwards condition or the affine-deformation condition). However, this change does not affect eqs 20−22, 29, and 30 deduced for the *normalized* viscoelastic and dielectric quantities of the chains in the dilated tube. Hereafter, we utilize $N = G_N/\nu k_B T$ for the affine deformation to specify the entanglement density in the system.

4.1 Monodisperse Systems. Figures 2 and 3 show the G* and ϵ'' data at 40 °C obtained for the entangled, monodisperse bulk PI systems with $10^{-3}M = 48.8$ and 94.0. The number of entanglements per chain, $N = M/M_e$, is 9.8 and 18.8, respectively ($M_e = 5 \times 10^3$ for bulk PI).[1] The G* data are normalized by the entanglement plateau modulus, G_N, and the ϵ'' data, by the dielectric relaxation intensity $\Delta\epsilon$ due to the global PI motion. For more heavily entangled PI system with $M = 140 \times 10^3$ ($N = 28$) and $M_w/M_n = 1.05$, we similarly normalized the G'' and ϵ'' data (at 0 °C) reported by Adachi et al.[28] (No G' data were reported.) The results are shown in Figure 4.

The PI chains have so-called type-B dipoles[20,28] perpendicular to the chain backbone, and the local mode referred to as the α-dispersion is dielectrically observed. However, this dispersion emerges at high ω not covered for the ϵ'' data shown in Figures 2−4. Thus, these data exclusively reflect the global chain motion (that is dielectrically active because of the type-A dipoles).

In contrast, the G'' data (at 40 °C) shown in Figures 2 and 3 have considerable contributions from fast viscoelastic modes (the so-called glass-to-rubber transition (GRT) modes) at $\omega > 10^3$ s^{-1}. However, at $\omega < 10^3$ s^{-1}, the data are negligibly contributed from the GRT modes and exclusively attributable to the global chain motion. Similarly, the G'' data of the high-M PI *at 0 °C* (Figure 4) have a negligible GRT contribution at $\omega < 10^{1.5}$ s^{-1}.

At such low ω, the G'' and ϵ'' data exhibit significantly different ω dependencies; see unfilled squares and filled circles in Figures 2−4. The slow relaxation mode distribution, reflecting the global chain motion, is considerably broader for G'' than it is for ϵ''. This result indicates that the relationship for the case of the fixed tube, $G''(\omega)/G_N = \epsilon''(\omega)/\Delta\epsilon$ (derived from eq 7), does not hold for the monodisperse PI chains with $10 \le M/M_e \le 30$. Thus, the tube is not fixed for these well-entangled chains.

For the PI chains with $10^{-3}M = 48.8$ and 94.0, the dielectric spectrum $\{g_p, \tau_p\}$ appearing in eq 20 was determined with the previously reported iteration method.[29] A constant interval of the relaxation times in the logarithmic scale was assumed, $\log[\tau_p/\tau_{p+1}] = \Delta$ ($p = 1, 2,...$). For various Δ values chosen in the range of $\Delta < 0.3$, the resulting spectra reproduced the ϵ'' data with equally high accuracy. This nonuniqueness is well-known for the empirical evaluation of spectra.[29] However, the G* calculated from eqs 21 and 22 for different dielectric spectra (for different Δ values < 0.3) were indistinguishable, and the nonuniqueness did not disturb our test for the molecular picture of tube dilation.

In Figures 2 and 3, the $\epsilon''(\omega)/\Delta\epsilon$ (eq 20) recalculated from the dielectric spectra with $\Delta = 0.1$ are shown with the dotted curves, and the $G^*(\omega)/G_N$ (eqs 21 and 22) calculated from the same spectra are indicated with the solid curves. For the high-M PI sample shown in Figure 4, Adachi et al.[28] reported the dielectric spectrum with $\Delta = 0.1$. The $\epsilon''(\omega)/\Delta\epsilon$ and $G''(\omega)/G_N$ similarly calculated from this spectrum are shown in Figure 4 (dotted and solid curves).

For all PI systems examined, the calculated $G^*(\omega)/G_N$ are close to the data at low ω where the fast GRT modes negligibly contribute to the data, although detailed inspection indicates some differences (e.g., the difference in the observed and calculated G'' peak location; cf. Figure 4). This result strongly suggests the (approximate) validity of the DTD molecular picture at those ω.

In Figures 2 and 3, the GRT contribution disturbs the comparison of the observed and calculated $G^*(\omega)/G_N$ at high ω ($>10^3$ s^{-1}). In principle, the comparison can be made after subtracting this contribution from the data. However, the functional form (ω dependence) of the GRT contribution is still controversial: The simplest idea is to use the Rouse relaxation modulus for the entanglement strand of the molecular weight M_e, but there is a possibility that the Rouse relaxation extends to the whole chain (as considered in the Milner−McLeish model[15]). Thus, in this paper, we do not attempt to make this subtraction. Instead, at high $\omega > 10^3$ s^{-1}, we just compare the observed and calculated G'/G_N that is much less sensitive to the fast GRT modes than G''/G_N. Good agreement is noted for the observed and calculated G'/G_N at ω up to 10^5 s^{-1}. Thus, the relationship deduced for the chain in the dilated tube, eqs 19−22 (with $\alpha = 1$), is approximately valid in a rather wide range of time/

frequency for the monodisperse PI having $M/M_e = 10-30$.

It should be also emphasized that the above validity of eqs 19−22 just suggests that the tube dilates in the time scale of the chain relaxation. In other words, this validity does not necessarily mean that the chain reptates along the dilated tube with its intrinsic curvilinear diffusion coefficient, D_c ($= N\zeta/k_BT$). The nonreptative motion in the dilated tube (that satisfies eqs 19−22) is found, for example, in the model by Viovy et al.:[19] In the chain reptation regime in their model, the chain reptates with D_c along the thin (nondiluted) tube of diameter a, and this thin tube fluctuates in the dilated tube ("supertube" in their terminology). Viscoelastic relaxation attributable to this type of chain motion was observed by Struglinski and Graessley for polybutadiene (PB) blends.[30]

For examination of the chain motion in the dilated tube, we estimated the ratio of the global CR relaxation time τ_{CR} ($\propto M^5$ in the monodisperse systems)[9,10,18] to the observed relaxation time τ_{obs} ($\propto M^{3.5}$). For the PI sample with $M = 48.8 \times 10^3$, the ratio was roughly estimated (from PI/PI blends data[31]) to be $\tau_{CR}/\tau_{obs} \cong 3.5$.[22] From this ratio, we may estimate $\tau_{CR}/\tau_{obs} \cong 9.4$ and 17 for $10^{-3}M = 94$ and 140. These results suggest that the terminal relaxation is faster than the global CR relaxation for the three PI samples examined in Figures 2−4. The reptation in the dilated tube would occur only after the chain contour length measured along this tube is equilibrated via the global CR mode, i.e., at $t > \tau_{CR}$, as suggested from viscoelastic data of blends.[18] Thus, the motion of the PI chains examined in Figures 2−4 may be more or less similar to that considered in the model by Viovy et al.[19] However, their model does not incorporate the contour length fluctuation (CLF) mechanism and its prediction for τ_{max} is quantitatively different from the experimental results.[18] In addition, the τ_{CR}/τ_{obs} ratio is not significantly larger than unity ($\tau_{CR}/\tau_{obs} \cong 17$ even for the highest-M PI examined), and we cannot completely rule out the possibility of the reptation (with CLF) along the dilated tube. Further studies are necessary for the details of the chain motion in the dilated tube.

4.2 Dilute PI Probe in Blends. The ϵ_2'' and G_2^* data[22,23,27] are available for the dilute PI probe ($M_2 = 48.8 \times 10^3$, $\upsilon_2 = 0.05$) in high- and low-M linear PB matrices with $10^{-3}M_1 = 9.24$ and 263 ($M/M_e = 5.0$ and 142; $M_e = 1.85 \times 10^3$ for bulk PB[30]). The matrix PB chains have no type-A dipoles. Thus, the G_2^* data are expected to be described by eqs 29 and 30 *if* the tube dilates in the time scale of the probe relaxation. This expectation is examined below.

As we did for the monodisperse PI systems, we utilized the ϵ_2'' data[22,27] to determine the dielectric spectrum $\{g_p, \tau_p\}$ of the PI probe. For evaluation of the relaxation times and intensities $\tau_{r,q}$ and r_q for $[\mu_{1,m}(t)]^{1/2}$ of the pure PB matrices, we converted the G^* data[23] of these matrices into $G(t)$ with the method of Ferry,[1]

$$G(t) \cong [G'(\omega) - 0.40G''(0.40\omega) + 0.014G''(10\omega)]_{\omega=1/t} \quad (31)$$

Figure 5 shows the $[\mu_{1,m}(t)]^{1/2} = [G(t)/G_N]^{1/2}$ thus obtained (symbols). Fitting these $[\mu_{1,m}(t)]^{1/2}$ data with a sum of exponentially decaying terms, we determined $\tau_{r,q}$ and r_q. The solid curves indicate the $[\mu_{1,m}(t)]^{1/2}$ recalculated from these $\tau_{r,q}$ and r_q.

In Figure 6, the G_2^*/G_{N_2} data[23] for the dilute PI probe

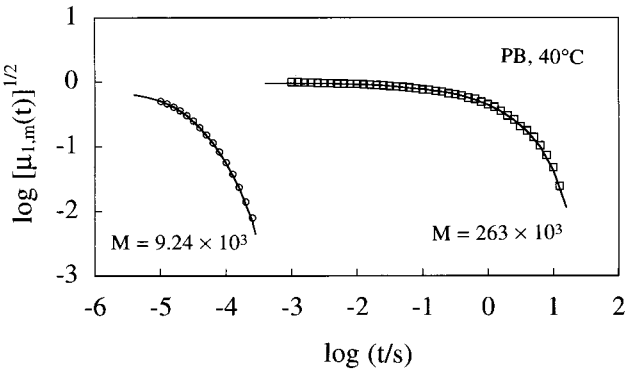

Figure 5. Square root of the normalized relaxation moduli, $[\mu_{1,m}(t)]^{1/2} = [G(t)/G_N]^{1/2}$, of two monodisperse PB at 40 °C. These PB are utilized as matrices of the blends examined in Figure 6.

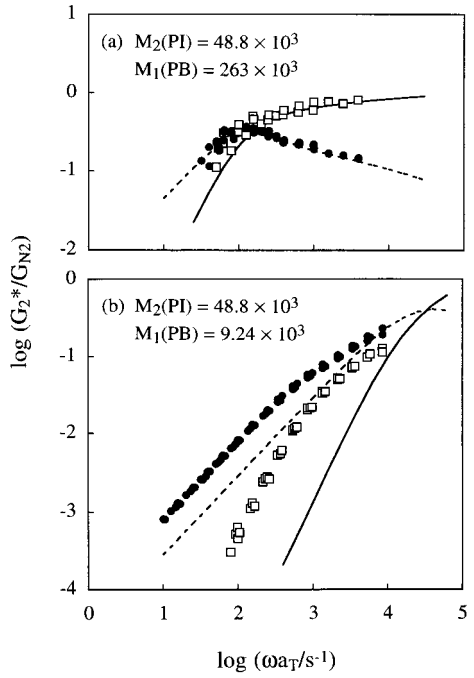

Figure 6. Comparison of normalized viscoelastic moduli G_2^*/G_{N_2} of dilute PI probe ($M_2 = 48.8 \times 10^3$, $\upsilon_2 = 0.05$) in entangling matrices of high- and low-M linear PB chains ($10^{-3}M_1 = 9.24$ and 263) at 40 °C[23] with the moduli calculated from the dielectric spectra for the case of tube dilation (eqs 29 and 30). The G_2'/G_{N_2} and G_2''/G_{N_2} data are shown with the unfilled squares and filled circles, respectively, and the calculated G_2'/G_{N_2} and G_2''/G_{N_2} with the solid and dotted curves, respectively. (The normalized relaxation moduli of the matrices, utilized in the calculation, are shown in Figure 5.) In the high-M matrix that hardly relaxes in the time scale of the probe PI relaxation, the calculated G_2^*/G_{N_2} is very close to that for the case of no tube dilation. For more details, see text.

are compared with the G_2^*/G_{N_2} calculated from g_p, τ_p, r_q, and $\tau_{r,q}$ determined above. The data (symbols), obtained by subtracting the matrix PB contribution from G^* of the PI/PB blends, are shown only at low ω where the uncertainties due to the subtraction are acceptably small.[23] At such low ω, the glass-to-rubber transition modes have no contributions to the G_2^*/G_{N_2} data. Thus, the data exclusively reflect the global motion of the dilute PI probe in the PB matrices.

In the PB matrices, the entanglement spacing for the dilute PI probe was found to be $M_{e,2} \cong 1.7 \times 10^3$.[23] Thus, the PI probe examined in Figure 6 has $N_2 = M_2/M_{e,2} \cong 28.7$ and is in a well-entangled state. Nevertheless, the

G_2^*/G_{N_2} data are quite different in the two matrices. This difference reflects a different contribution of the constraint release (CR) mechanism in these matrices: The τ_{CR}/τ_{obs} ratio is 5600 for the PI probe in the high-M PB matrix, and thus, the probe relaxation is much faster than the CR relaxation; namely, the CR mechanism has a negligible contribution to the probe relaxation in this matrix.[23] In contrast, the PI probe in the low-M matrix has $\tau_{CR}/\tau_{obs} = 1.1$, and its relaxation is dominated by the CR mechanism.[23]

As noted in Figure 6a, the G_2^*/G_{N_2} data (symbols) in the high-M matrix coincide with the G_2^*/G_{N_2} calculated from eqs 29 and 30 (curves). In this matrix, $[\mu_{1,m}(t)]^{1/2}$ hardly decays, and the tube diameter (determined by this $\mu_{1,m}$) does not increase in the time scale of the probe relaxation ($t \leq 10^{-2}$ s, or $\omega \geq 10^2$ s^{-1}); see Figure 5. The above coincidence of the observed and calculated G_2^*/G_{N_2} reflects this lack of tube dilation. In fact, the relationship $G_2''/G_{N_2} = \epsilon_2''/\Delta\epsilon$ derived from eq 28 with $[\mu_{1,m}(t)]^{1/2} = 1$ (no dilation case) was confirmed for the viscoelastic and dielectric data of the probe in the high-M matrix.[23] All of these results are consistent with the CR-free nature of the probe relaxation in this matrix ($\tau_{CR}/\tau_{obs} = 5600 \gg 1$): Because the tube dilates as a result of the CR motion of the probe, no dilation occurs in the CR-free environment.

In the low-M matrix (Figure 6b), the CR mechanism dominates the probe relaxation,[22,23] and the tube can dilate *in principle*. Nevertheless, the G_2^*/G_{N_2} calculated for the case of tube dilation (eqs 29 and 30) is significantly different from the data. Specifically, the calculated probe relaxation is considerably faster than the data: The terminal relaxation time $\langle\tau_2\rangle_w = [G_2'/\omega G_2'']_{\omega\to 0}$ is 5×10^{-5} s for the calculation and 7×10^{-4} s for the data. These results demonstrate the importance of the mutual equilibration of the entanglement segments of the probe,[18] as explained below.

The tube dilation process includes two steps: the removal of the constraints due to diffusion of the matrix chains and the CR motion of the probe chain activated by this removal. This CR motion results in the above equilibration of the probe segments and allows the tube to dilate. The model (eq 26) assumes that the CR equilibration completes immediately and the tube dilates instantaneously on the removal of the constraints. (The factor $[\mu_{1,m}(t)]^{1/2}$ in eq 26 reflects this assumption.) However, the actual CR motion requires a characteristic time $\sim \beta^2 t_w$, where t_w is the entanglement lifetime determined by the matrix diffusion and β is the number of the probe entanglement segments involved in this motion. Thus, the tube diameter increases to $a' = \beta^{1/2}a$ only at $t \geq \beta^2 t_w$. This difference between the model assumption and the behavior of the actual probe leads to the difference of the observed and calculated G_2^* in Figure 6b. In fact, our previous studies[22,23] demonstrated that the dilute probe in the low-M matrix relaxes completely via the CR mechanism during the equilibration process.

5. Concluding Remarks

For viscoelastic and dielectric properties of chains having noninverted type-A dipoles, we have derived a specific relationship that should be valid when the tube dilates in time scale of the chain relaxation. This relationship was found to be approximately valid for monodisperse PI chains with $M/M_e = 10-30$. This result suggests the importance of tube dilation for the terminal relaxation of these PI chains, although the chains do not necessarily reptate along the dilated tube with their intrinsic curvilinear diffusion coefficient.

In contrast, for dilute probe PI chain in the low-M entangling PB matrix, the relationship was not valid. This result indicates that the probe fully relaxes via the CR mechanism during the mutual equilibration of its entanglement segments, demonstrating the importance of the CR motion of the probe in the tube dilation process. The lack of the tube dilation was also confirmed for the probe in the high-M PB matrix where the CR mechanism negligibly contributed to the probe relaxation.

Acknowledgment. We acknowledge, with thanks, financial support to this work from the Ministry of Education, Science, Culture, and Sports, Japan (Grant No. 10450366) and from Japan Chemical Innovation Institute (through the Doi Project for development of Platform for designing high functional materials).

References and Notes

(1) Ferry, J. D. *Viscoelastic Properties of Polymers*, 3rd ed.; Wiley: New York, 1980.
(2) Graessley, W. W. *Adv. Polym. Sci.* **1974**, *16*, 1.
(3) Doi M.; Edwards, S. F. *J. Chem. Soc., Faraday Trans. 2* **1978**, *74*, 1789, 1802, 1818.
(4) Doi M.; Edwards, S. F. *The Theory of Polymer Dynamics*; Clarendon: Oxford, 1986.
(5) Doi, M.; Kuzuu, N. *J. Polym. Sci., Polym. Lett. Ed* **1980**, *18*, 775.
(6) Pearson, D. S.; Helfand, E. *Macromolecules* **1984**, *17*, 888.
(7) Doi, M. *J. Polym. Sci., Polym. Lett. Ed.* **1981**, *19*, 265.
(8) Doi, M. *J. Polym. Sci., Polym. Phys. Ed.* **1983**, *21*, 667.
(9) Klein, J. *Macromolecules* **1978**, *11*, 852.
(10) Graessley, W. W. *Adv. Polym. Sci.* **1982**, *47*, 68.
(11) Marrucci, G. *J. Polym. Sci., Polym. Phys. Ed.* **1985**, *23*, 159.
(12) Ball, R. C.; McLeish, T. C. B. *Macromolecules* **1989**, *22*, 1911.
(13) Milner, S. T.; McLeish, T. C. B. *Macromolecules* **1997**, *30*, 2159.
(14) Milner, S. T.; McLeish, T. C. B. *Macromolecules* **1998**, *31*, 7479.
(15) Milner, S. T.; McLeish, T. C. B. *Phys. Rev. Lett.* **1998**, *81*, 725.
(16) Rubinstein, M.; Helfand, E.; Pearson, D. S. *Macromolecules* **1987**, *20*, 822.
(17) Rubinstein, M.; Colby, R. H. *J. Chem. Phys.* **1988**, *89*, 5291.
(18) Watanabe, H. *Prog. Polym. Sci.*, in press.
(19) Viovy, J. L.; Rubinstein, M.; Colby, R. H. *Macromolecules* **1991**, *24*, 3587.
(20) Stockmayer, W. H. *Pure Appl. Chem.* **1967**, *15*, 539.
(21) Watanabe, H.; Yao, M.-L.; Osaki, K. *Macromolecules* **1996**, *29*, 97.
(22) Matsumiya, Y.; Watanabe, H.; Osaki, K.; Yao, M.-L. *Macromolecules* **1998**, *31*, 7528.
(23) Watanabe, H.; Matsumiya, Y.; Osaki, K.; Yao, M.-L. *Macromolecules* **1998**, *31*, 7538.
(24) Janeschitz-Kriegl, H. *Polymer Melt Rheology and Flow Birefringence*; Springer: Berlin, 1983.
(25) Cole, R. H. *J. Chem. Phys.* **1965**, *42*, 637.
(26) Watanabe, H.; Urakawa, O.; Kotaka, T. *Macromolecules* **1993**, *26*, 5073.
(27) Watanabe, H.; Urakawa, O.; Kotaka, T. *Macromolecules* **1994**, *27*, 3525.
(28) Adachi, K.; Yoshida, H.; Fukui, F.; Kotaka, T. *Macromolecules* **1990**, *23*, 3138.
(29) Yoshida, H.; Adachi, K.; Watanabe, H.; Kotaka, T. *Polym. J.* **1989**, *21*, 863.
(30) Struglinski, M. J.; Graessley, W. W. *Macromolecules* **1985**, *18*, 2630.
(31) Adachi, K.; Itoh, S.; Nishi, I.; Kotaka, T. *Macromolecules* **1990**, *23*, 2554.

MA991121Q